### Original Article

# WSB1 promotes prostate cancer malignancy through OTUD4-mediated ISOC2 stabilization and P16INK4a suppression

Jian Sun<sup>1,2</sup>, Fei Wang<sup>2</sup>, Yuxuan Feng<sup>3</sup>, Xiya Qiu<sup>3</sup>, Wenying Qu<sup>3</sup>, Xuefeng He<sup>1</sup>, Jianjun Xie<sup>2</sup>, Gang Li<sup>1</sup>

<sup>1</sup>Department of Urology, The First Affiliated Hospital of Soochow University, Suzhou 215000, Jiangsu, China; <sup>2</sup>Department of Urology, The Affiliated Suzhou Hospital of Nanjing Medical University, Suzhou Municipal Hospital, Gusu School, Nanjing Medical University, Suzhou 215002, Jiangsu, China; <sup>3</sup>State Key Laboratory of Reproductive Medicine and Offspring Health, Center for Reproduction and Genetics, The Affiliated Suzhou Hospital of Nanjing Medical University, Suzhou Municipal Hospital, Gusu School, Nanjing Medical University, Suzhou 215002, Jiangsu, China

Received September 2, 2025; Accepted October 21, 2025; Epub October 25, 2025; Published October 30, 2025

Abstract: Polyubiquitination plays a critical role in tumor biology, yet its significance in prostate cancer remains incompletely understood. Here, we investigated the expression and function of SOCS-box E3 ligases in prostate cancer. Analysis of TCGA data revealed WSB1 overexpression, which correlated with advanced pathological stage, high Gleason score, and poor prognosis. Functional assays demonstrated that WSB1 knockdown suppressed prostate cancer cell proliferation, colony formation, and migration in vitro, and inhibited tumor growth and Ki67 expression in vivo. Mechanistically, mass spectrometry and co-immunoprecipitation identified ISOC2 as a key WSB1 interactor. WSB1 stabilized ISOC2 by promoting its interaction with the deubiquitinase OTUD4, thereby preventing ISOC2 degradation via the ubiquitin-proteasome pathway. Silencing either ISOC2 or OTUD4 phenocopied the tumor-suppressive effects of WSB1 ablation. Importantly, disruption of the WSB1/OTUD4/ISOC2 axis upregulated P16INK4a expression, and co-silencing of P16INK4a partially restored tumorigenic properties. Our findings unveil a novel WSB1/OTUD4/ISOC2 signaling network that drives prostate cancer progression by modulating ubiquitin signaling and repressing P16INK4a, positioning WSB1 as a promising therapeutic target.

Keywords: WSB1, prostate cancer, ubiquitination, OTUD4, ISOC2

#### Introduction

Prostate cancer, classified as a malignant tumor originating from the epithelium of the prostate gland, has been reported as the most frequently diagnosed malignancy among men. With early symptoms frequently absent, regional lymph-node metastases are identified in approximately 14% of patients at diagnosis and distant metastases in approximately 10%; among the latter, a 5-year survival of only 37% has been reported [1, 2]. Although androgen deprivation therapy (ADT) was initially considered effective, disease progression to castration-resistant prostate cancer (CRPC) has been observed in 10%-20% of patients within five years. Among these, metastases have occurred in as many as 15%-33%, contributing to a

markedly poor prognosis [3]. Increased tumor aggressiveness associated with neuroendocrine differentiation (NED), resistance induced by activation of androgen receptor signaling bypass pathways, and immune escape resulting from suppression of the immune microenvironment have all been extensively demonstrated; however, targeted therapeutic strategies with durable efficacy remain lacking [4-6]. In light of these significant clinical challenges, the identification of more reliable molecular markers and the elucidation of deeper mechanistic insights are urgently required to support precise disease stratification and personalized treatment approaches.

The ubiquitin-proteasome system (UPS) is regarded as the principal proteolytic machinery

responsible for maintaining intracellular protein homeostasis, mediating the selective degradation of more than 80% of cellular proteins through a cascade consisting of E1 activation, E2 conjugation, and E3 ligase-mediated polyubiquitination, followed by 26S proteasomedependent proteolysis [7-11]. Disruption of UPS fidelity has emerged as a hallmark of prostate tumorigenesis, wherein hyperactivation of specific E3 ligases accelerates the turnover of tumor suppressors such as PTEN and p53, while aberrant stabilization of oncogenic effectors including the androgen receptor (AR) and B-catenin drives cellular proliferation and therapy resistance [12, 13]. Among E3 ligases, a significant subset functions through multicomponent complexes, such as the ECS (Elongin-Cullin-SOCS-box) E3 ligase family. This family comprises 41 SOCS-box-containing proteins in humans, which serve as substrate recognition subunits within ECS complexes assembled from Elongin B/C (ELOB/ELOC), Cullin 2 or 5 (CUL2/5), and RING-box proteins (RBX1/2) [14]. The SOCS-box domain facilitates the recruitment of the Elongin-Cullin scaffold and dictates substrate specificity, thereby determining the target selectivity of the ubiquitination machinery [14]. WSB1, a WD-repeat and SOCS-box containing E3 ligase adaptor, is notably upregulated in aggressive prostate cancer and strongly associated with poor clinical outcomes. Mechanistically, WSB1 has been demonstrated to exert dual oncogenic activities. Within the canonical UPS pathway, it has been reported to promote degradation of the tumor suppressor NKX3.1 and to enhance hypoxia adaptation through stabilization of HIF- $1\alpha$  [7, 15]. Intriguingly, emerging evidence implicates WSB1 in non-proteolytic regulatory circuits, including WSB1 affected β-catenin destruction complex-PPP2CA assembly and E3 ubiquitin ligase adaptor β-TRCP recruitment, which inhibited the ubiquitination of β-catenin and transactivated c-Myc [16]. However, the molecular basis of these UPS-independent activities remains largely undefined. A comprehensive proteomic dissection of the WSB1 interactome and downstream effector networks may uncover previously unrecognized substrate recognition motifs and post-translational modification crosstalk, offering mechanistic insight into its multifaceted role in prostate cancer progression and a potential framework for therapeutic intervention.

In this study, the expression profile and prognostic significance of genes involved in polyubiquitination in prostate cancer were systematically investigated, and the E3 ubiquitin ligase WSB1 was identified as a critical regulator of tumor progression. Elevated expression of WSB1 in high-grade tumors, along with its essential role in maintaining tumor cell viability, was demonstrated through immunofluorescence and functional assays. Through coimmunoprecipitation followed by mass spectrometry, ISOC2 and OTUD4 were identified as novel interacting partners of WSB1. Mechanistically, WSB1 was found to function as a scaffold that stabilizes the interaction between OTUD4 and its substrate ISOC2. Knockdown of WSB1 disrupted this complex, resulting in increased ubiquitination and proteasomal degradation of ISOC2, thereby impairing the downstream regulation of the tumor suppressor P16INK4a. Notably, silencing of P16INK4a was shown to partially rescue the reduction in cell viability induced by WSB1 knockdown. These findings uncover a previously unrecognized WSB1-OTUD4-ISOC2-P16-INK4a regulatory axis that promotes prostate cancer progression and provide a mechanistic rationale for targeting WSB1 as a potential therapeutic strategy.

#### Materials and methods

#### Bioinformatics analysis

A total of 41 SOCS-box-containing proteins from nine different families have been recognized to regulate protein turnover by targeting substrates for polyubiquitination and subsequent proteasome-mediated degradation [14]. The expression profiles of 41 polyubiquitination-related genes were downloaded from the TCGA database and analyzed for differential expression between prostate cancer and adjacent normal tissues using the "Limma" package. Kaplan-Meier survival analyses for the WSB1 and VHL genes were performed using the "survival" and "survminer" packages to evaluate overall survival (OS) [17].

#### Immunofluorescence

Immunofluorescence assays were performed as described previously [18, 19]. Briefly, paraffin-embedded tissue sections were deparaffinized in xylene and rehydrated through graded

ethanol. Antigen retrieval was performed in 10 mM citrate buffer (pH 6.0) using microwave heating. After cooling, sections were permeabilized with 0.1% Triton X-100 in PBS and blocked with 5% BSA for 30 minutes. Slides were then incubated overnight at 4°C with primary antibodies (anti-WSB1, Proteintech; anti-Ki67, Abcam) diluted in blocking buffer. Following PBS washes, fluorescently labeled secondary antibodies were applied for 1 hour at room temperature in the dark. Nuclei were counterstained with 4',6-diamidino-2-phenylindole (DAPI). Finally, slides were mounted using anti-fade mounting medium and visualized using a confocal laser scanning microscope (LSM800, Carl Zeiss, Germany).

#### Cell culture and transfection

Prostate cancer cell lines (PC-3 and DU145) were obtained from the Cell Bank of the Chinese Academy of Sciences (Shanghai, China). Cells were cultured in RPMI-1640 medium (Gibco, USA) supplemented with 10% fetal bovine serum (Gibco, Australia) in a humidified incubator containing 5% CO<sub>2</sub> at 37°C. Small interfering RNAs (siRNAs) targeting WSB1, ISOC2, OTUD4, and P16INK4a, along with the negative control siRNA (si-NC), were transfected into DU145 and PC-3 cells using Lipofectamine 2000 (Invitrogen, USA) according to the manufacturer's protocol. The nucleotide sequences of the siRNAs were as follows: si-WSB1#1: 5'-GAAAGAGAUCGUGAGAUU-ACG-3': si-WSB1#2: 5'-CGUACUAUAGGUGAA-CUUUUA-3'; si-ISOC2#1: 5'-GCAGAAUAAACAU-AUAUGUGG-3'; si-ISOC2#2: 5'-GGCCGUCCGA-GAGCCGAGAGG-3'; si-OTUD4#1: 5'-CUCGAAA-GCCCGCAAAUUAAC-3': si-OTUD4#2: 5'-CUGU-AUUCACUAUCUUCGAGA-3'; si-P16INK4a: GC-UUUCGUAGUUUUCAUUUAG; si-NC: 5'-UUCUCC-GAACGUGUCACGU-3'. In addition, sh-WSB1 and negative control (sh-NC) (GenePharma, Suzhou, China) were stably transfected into PC-3 cells. The overexpression plasmid pc-DNA3.1-WSB1 and the corresponding empty vector (EV) were synthesized by GenePharma and transfected using Lipofectamine 2000. Cells were collected 48 hours post-transfection for further analysis.

RNA extraction and quantitative reverse-transcription PCR (qRT-PCR)

Total RNA was isolated from cultured cells using TRIzol reagent (Thermo Fisher Scientific,

USA) following the manufacturer's instructions. RNA quality was assessed using a NanoDrop spectrophotometer. cDNA was synthesized from 1 µg of RNA using the HiScript III RT SuperMix kit (Vazyme, Nanjing, China). Quantitative PCR was performed using ChamO Universal SYBR qPCR Master Mix (Vazyme) on a StepOnePlus Real-Time PCR System (Applied Biosystems, USA). Gene expression was normalized to 18s rRNA expression and calculated based on the 2- $\Delta\Delta$ CT method. The following primers were used: WSB1 forward 5'-TCAACGAGAAAGAGATCGTGAGA-3', and reverse 5'-TGCGATGTCCTTGTGACCAA-3': ISOC2 forward 5'-GCCTGCATCTTGAACACGAC-3', and reverse 5'-GGAAGGCACCACTCTGTCTC-3': OT-UD4 forward 5'-TAACGGGGTGTCTCTCTCT-3', and reverse 5'-TTGTCCTACCCATTCCTGTGG-3'; P16INK4a forward 5'-GGAGGCCGATCCAGGT-CAT-3', and reverse 5'-CACCAGCGTGTCCAGG-AAG-3': and 18s rRNA, forward 5'-AAACGGC-TACCACATCCAAG-3' and reverse 5'-CCTCCAA-TGGATCCTCGTTA-3'.

#### Cell viability and migration assays

Cell proliferation was assessed using the Cell Counting Kit-8 (CCK-8, Beyotime, Nantong), as previously described [20, 21]. Briefly, transfected PC-3 and DU145 cells were seeded into 96-well plates at a density of 2×10³ cells per well in triplicate. At 0, 24, 48, and 72 hours, 10 µL of CCK-8 reagent was added to each well, followed by incubation at 37°C for 2 hours. Absorbance was measured at 450 nm using a microplate reader (Bio-Rad Model 680, Richmond, CA, USA) to evaluate cell viability.

For the colony formation assay, approximately 800 transfected PC-3 or DU145 cells were plated into 6-well plates (500 cells/well) and cultured in complete medium for two weeks. When visible colonies had formed, cells were fixed with 4% paraformaldehyde for 20 minutes and stained with 0.1% crystal violet for 15 minutes. Colonies containing more than 50 cells were manually counted under a light microscope. Each experiment was repeated in triplicate.

Cell migration capacity was evaluated using Transwell chambers (Corning, USA) with 8- $\mu$ m pore size (BD Biosciences, USA). After transfection, 3×10<sup>4</sup> PC-3 or DU145 cells in serumfree medium were seeded into the upper chambers, while the lower chambers were filled with

 $600~\mu L$  medium containing 10% FBS as a chemoattractant. After 24 hours of incubation at  $37^{\circ}C$ , non-invading cells on the upper membrane surface were removed with a cotton swab. The invaded cells on the lower surface were fixed in 4% paraformaldehyde and stained with 0.1% crystal violet. Cells in five randomly selected fields were counted under a microscope.

#### In vivo assays

To assess the effect of WSB1 knockdown on tumorigenicity *in vivo*, male BALB/c nude mice (4 weeks old) were purchased from the Experimental Animal Center of Nanjing Medical University. The mice were housed in a controlled environment with a 12-hour light/dark cycle, a constant temperature of  $22 \pm 2^{\circ}$ C, and relative humidity of  $50\% \pm 10\%$ . Standard laboratory rodent chow and autoclaved water were provided *ad libitum*.

PC-3 cells stably expressing sh-WSB1 or EV  $(1\times10^7~\text{cells}$  in 100 µL PBS) were subcutaneously injected into the flanks of each mouse (n = 6). Tumor growth was monitored every three days, and volume was calculated using the formula:  $0.5\times \text{length}\times \text{width}^2$ . After 15 days, mice were euthanized under carbon dioxide exposure followed by cervical dislocation, and tumors were excised, weighed, and photographed. Tumor sections were fixed with methanol/acetone, followed by incubation with Ki67 antibody (1:50; Proteintech, USA) to evaluate cell proliferation via immunostaining. All procedures were approved by the Animal Ethics Committee of Nanjing Medical University.

## Liquid chromatography-tandem mass spectrometry (LC-MS/MS)

Proteins interacting with WSB1 were separated by SDS-PAGE and visualized using a Fast Silver Stain Kit (Beyotime). Gel slices were excised, destained, and subjected to sequential washes with deionized water, 50% acetonitrile (ACN), and 100% ACN. After reduction with DTT and alkylation with IAA at room temperature, gels were dried and rehydrated in trypsin solution on ice for 30 minutes, then digested overnight at 37°C. Peptides were extracted, concentrated using a vacuum centrifuge, desalted with StageTips, and analyzed on an LTO Orbitrap Velos mass spectrometer (Thermo

Fisher). Data were searched against the UniProt human database with a 1% false discovery rate, and protein quantification was conducted using the iBAQ method embedded in MaxQuant software as described previously [22-24].

#### Immunoprecipitation (IP) assay

Cells were lysed in cold RIPA buffer (Beyotime, China) supplemented with protease inhibitors. After preclearing with Protein A magnetic beads (Invitrogen), the lysates were incubated overnight at 4°C with the indicated antibodies or control IgG (Proteintech) antibodies. Immune complexes were captured by incubation with Protein A beads for 3 hours. Following extensive washing to reduce non-specific binding, the complexes were eluted by boiling the beads in 2× SDS loading buffer at 95°C for 5 minutes. Eluted proteins were subsequently analyzed by Western blotting.

#### Western blotting

Total proteins were extracted using RIPA lysis buffer containing phosphatase and protease inhibitors, as previously described [25, 26]. Equal amounts of lysates were separated via SDS-PAGE and transferred onto PVDF membranes. After blocking with 5% skimmed milk in TBST for 1 hour, membranes were incubated overnight at 4°C with the following primary antibodies: anti-WSB1 (Proteintech, 1:1000), anti-OTUD4 (Proteintech, 1:1000), anti-ISOC2 (Abcam, 1:1000), anti-Flag (Sigma, 1:1000), and anti-Tubulin (Beyotime, 1:3000) as loading control. After washing, membranes were treated with HRP-conjugated secondary antibodies for 1 hour and developed using an enhanced chemiluminescence reagent (Thermo Scientific). Protein bands were detected with an enhanced chemiluminescent substrate (Thermo Scientific).

#### Statistical analysis

All statistical analyses were carried out using SPSS 22.0 (IBM, Chicago, IL, USA). Quantitative results were derived from at least three independent biological replicates and expressed as mean ± standard deviation (SD). Differences between two groups were assessed using a two-tailed Student's t-test, while one-way ANOVA followed by Tukey's post hoc was employed for comparisons involving more

than two groups. Survival outcomes were evaluated using the Kaplan-Meier method, and statistical differences between curves were determined with the log-rank test. All statistical tests were two-sided, with significance defined as P < 0.05.

#### Results

Comprehensive profiling of polyubiquitinationrelated genes reveals WSB1 as a key driver in prostate cancer

In the TCGA prostate cancer dataset, 25 out of 41 polyubiquitination-related genes were found to be significantly dysregulated in tumor tissues compared with adjacent normal tissues, suggesting a potential oncogenic role for polyubiquitination in prostate carcinogenesis. Specifically, the expression of SOCS1, SOCS3, SOCS5, SOCS6, ASB1, ASB2, ASB3, ASB4, ASB5, ASB8, ASB12, SPSB1, SPSB4, RAB40A, and NEURL1 was significantly downregulated in tumor tissues, whereas ASB13, ASB14, WSB1, WSB2, SPSB3, RAB40C, NEURL2, VHL, TULP4, and ELOA were upregulated (Figure 1A). Among the upregulated genes, WSB1 and VHL exhibited distinct and elevated expression patterns in prostate tumors, with high expression of either gene significantly correlated with poorer overall survival (OS) (Figure1B, 1C). While VHL is a well-characterized tumor suppressor gene whose functional loss leads to HIF accumulation and activation of pro-angiogenic (e.g., VEGF), glycolytic, and proliferative pathways [27], its elevated mRNA expression in tumors appeared inconsistent with its expected functional role. In contrast, the precise role and molecular mechanism of WSB1 in prostate cancer remains incompletely understood, thereby warranting further investigation. In the TCGA cohort, WSB1 demonstrated moderate diagnostic discrimination as a single biomarker (AUC = 0.609) (Figure 1D) and its expression was significantly associated with pathological T/N stage and Gleason score, suggesting a potential role in tumor progression (Figure 1E-G). Additionally, immunofluorescence staining revealed that WSB1 protein expression was markedly increased in prostate cancer tissues compared with normal controls (Figure 1H, 1I). The fluorescence intensity of WSB1 exhibited a stepwise increase in parallel with higher Gleason scores (Figure 1J, 1K), further supporting its relevance to tumor aggressiveness.

Functional characterization of WSB1 as an oncogenic driver in prostate cancer progression

To elucidate the functional role of WSB1 in prostate cancer progression, siRNA-mediated knockdown experiments were conducted in DU145 and PC-3 cell lines. As shown in Figure 2A, WSB1 mRNA expression was significantly reduced following transfection with two independent siRNAs (si-WSB1 1# and si-WSB1 2#), confirming effective gene silencing (Figure 2A). Cell proliferation assays demonstrated that WSB1 knockdown significantly suppressed cell viability in a time-dependent manner in both DU145 and PC-3 cells (Figure 2B, 2C). Consistently, colony formation assays showed a significant reduction in the number of colonies formed by WSB1-deficient cells, indicating impaired long-term proliferative capacity (Figure 2D, 2E). Furthermore, transwell migration assays revealed that WSB1 knockdown led to a marked decrease in the number of migrated cells in both cell lines compared to controls (Figure 2F, 2G). Collectively, these findings indicate that WSB1 is essential for sustaining the proliferative and migratory phenotypes of prostate cancer cells, supporting its potential role as an oncogenic driver in prostate tumor progression.

To further validate the oncogenic role of WSB1, overexpression experiments were performed in DU145 and PC-3 prostate cancer cell lines. As shown in Figure 3A, 3B, WSB1 overexpression was found to significantly enhance cell proliferation in both cell lines. Furthermore, colony formation and transwell migration assays demonstrated that WSB1-overexpressing cells exhibited increased clonogenic ability and migratory potential compared with control cells (Figure 3C-F). Overall, these findings indicate that WSB1 overexpression significantly promotes the malignant phenotype of prostate cancer cells.

WSB1 knockdown suppresses tumor growth and proliferation in vivo

To evaluate the in vivo role of WSB1 in prostate cancer, a xenograft mouse model was established using PC-3 cells stably expressing either sh-NC or sh-WSB1. Tumor growth was signifi-

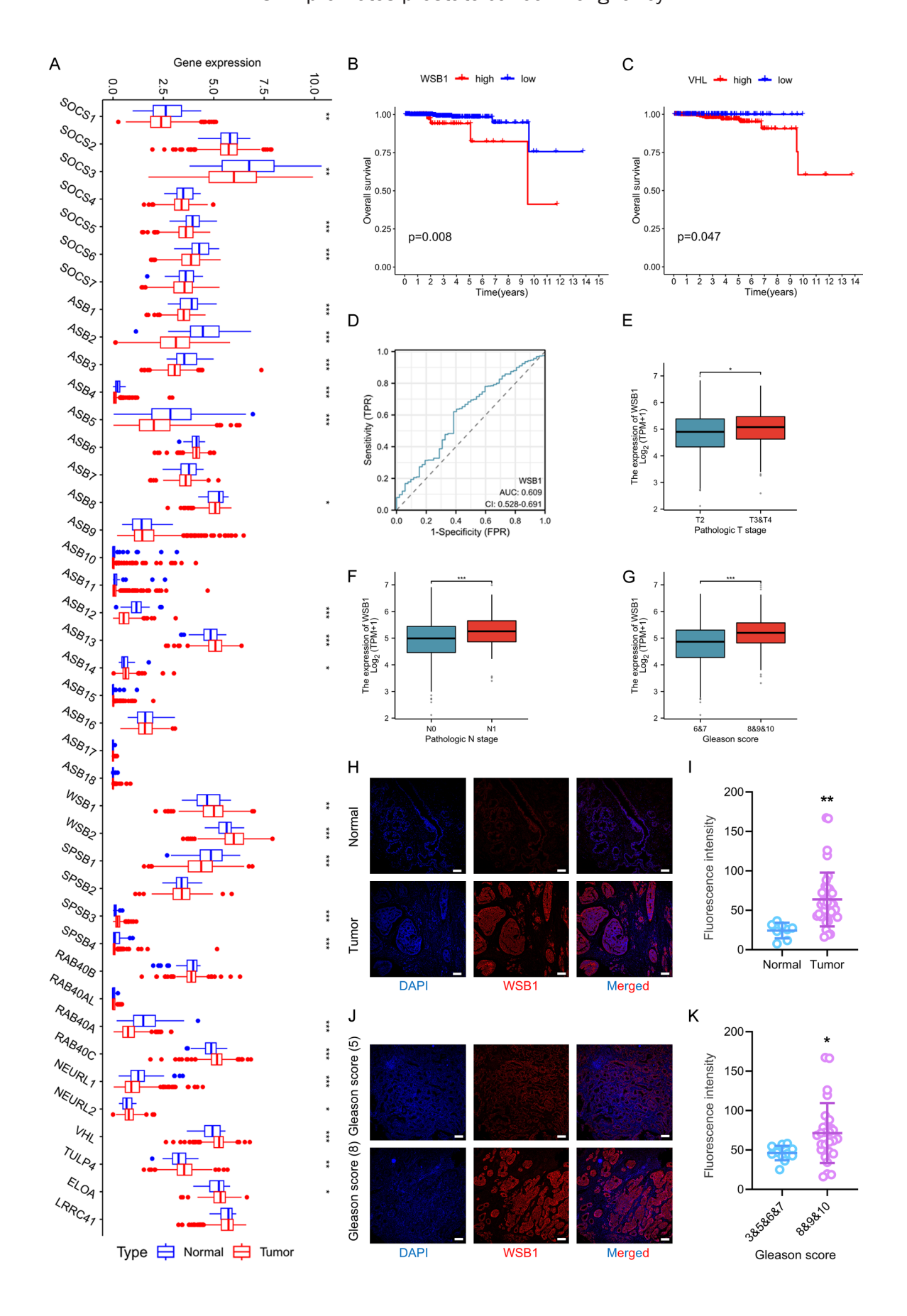


Figure 1. WSB1 overexpression correlates with gleason score and tumor progression in prostate cancer. A. In TCGA prostate cancer, 25 of 41 polyubiquitination genes were dysregulated in tumor versus adjacent normal tissues. B. High WSB1 expression was associated with significantly poorer overall survival compared to low expression levels. C. High VHL expression was associated with significantly poorer overall survival compared to low expression levels. D. WSB1 demonstrated moderate diagnostic discrimination as a single biomarker (AUC = 0.609). E-G. WSB1 expression showed significant association with pathological T/N stage and Gleason score in prostate cancer. H, I. WSB1 protein expression was markedly increased in prostate cancer tissues compared with normal controls. Bar: 100  $\mu$ m; magnification (×200). J, K. WSB1 exhibited a stepwise increase in parallel with higher Gleason scores. Bar: 100  $\mu$ m; magnification (×200). \*P < 0.05, \*\*P < 0.01, \*\*\*P < 0.001.

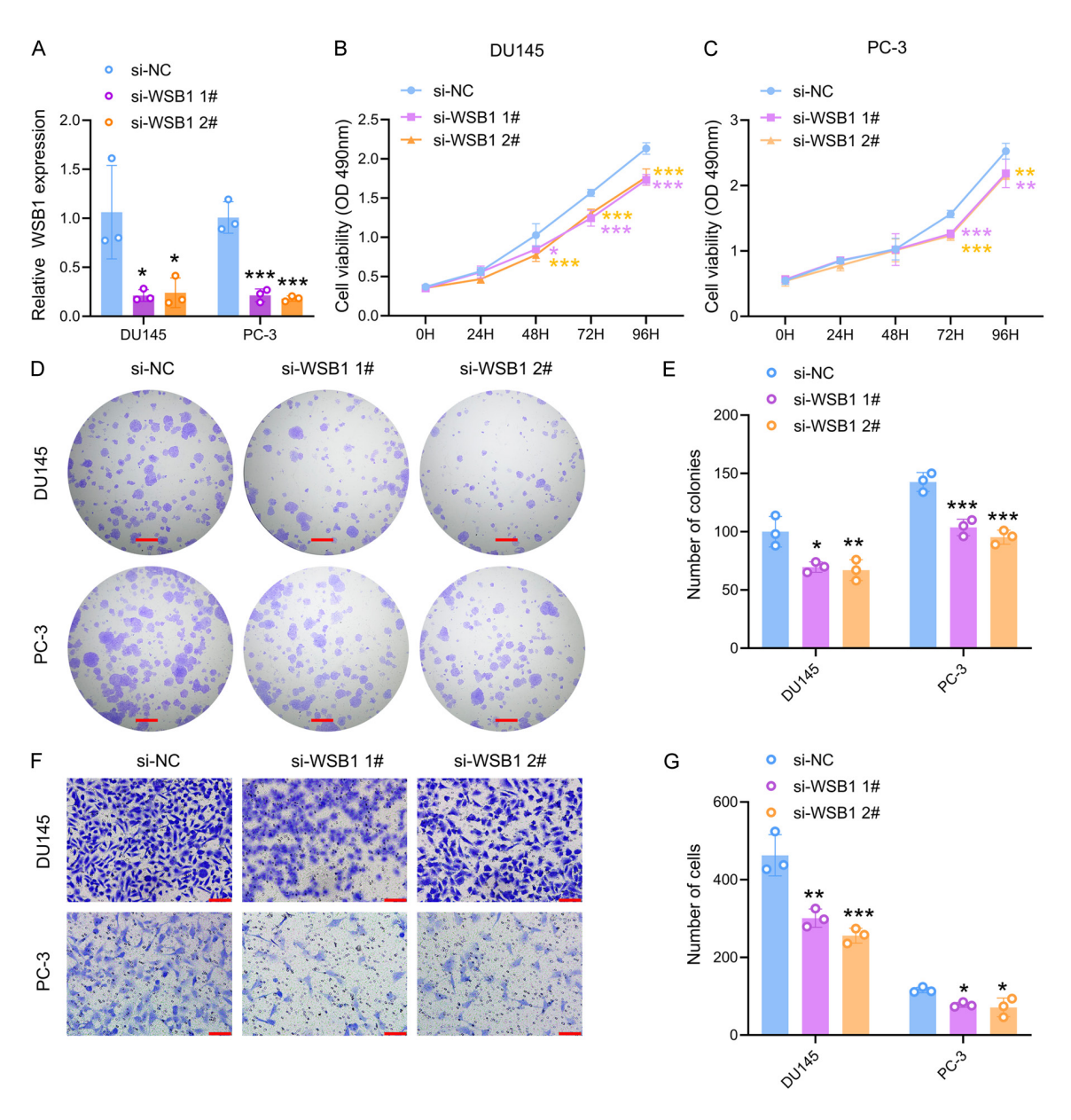


Figure 2. WSB1 knockdown impairs proliferation and migration in prostate cancer cells. A. Confirmation of WSB1 knockdown by RT-qPCR. n=3 per group. B, C. Cell proliferation assays demonstrated that WSB1 knockdown significantly suppressed cell viability in a time-dependent manner. n=6 per group. D, E. A significant reduction in the number of colonies formed by WSB1-deficient cells. n=3 per group. Bar: 2 mm; magnification (×1). F, G. WSB1 knockdown led to a marked decrease in the number of migrated cells in both cell lines. n=3 per group. Bar: 100  $\mu$ m; magnification (×200). \*P < 0.05, \*\*P < 0.01, \*\*\*P < 0.001.

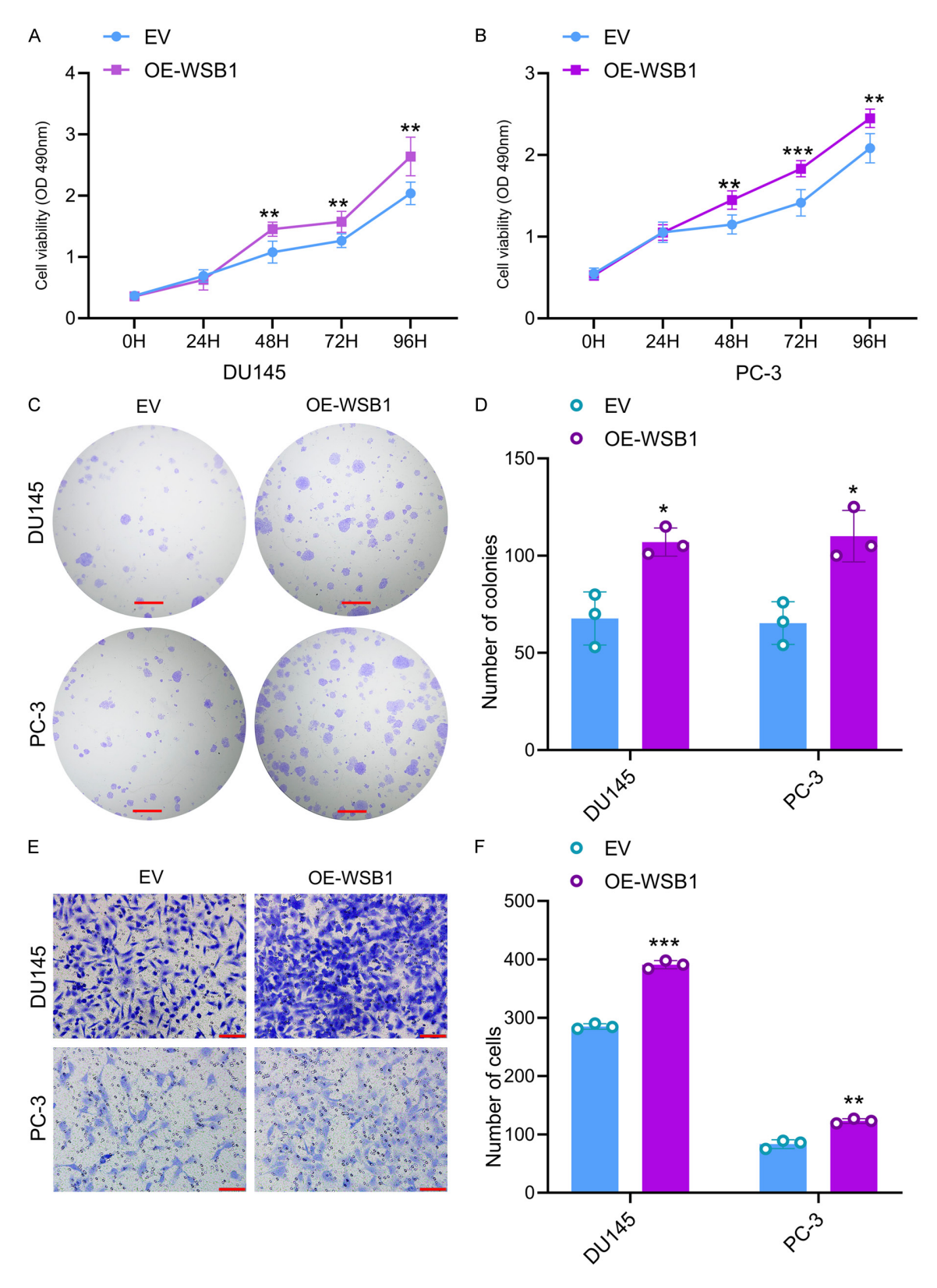


Figure 3. Impact of WSB1 overexpression on prostate cancer cell function. A, B. Cell viability was assessed in DU145 and PC-3 prostate cancer cell lines using CCK-8 assays following WSB1 overexpression (n = 6 per group). C, D. The capacity for colony formation was evaluated in DU145 and PC-3 cells overexpressing WSB1 using colony formation assays (n = 3 per group). Bar: 2 mm; magnification (×1). E, F. Cell migration was measured in DU145 and PC-3 cells with WSB1 overexpression using Transwell assays (n = 3 per group). Bar: 100  $\mu$ m; magnification (×200). \*P < 0.05, \*\*P < 0.01, \*\*\*P < 0.001.

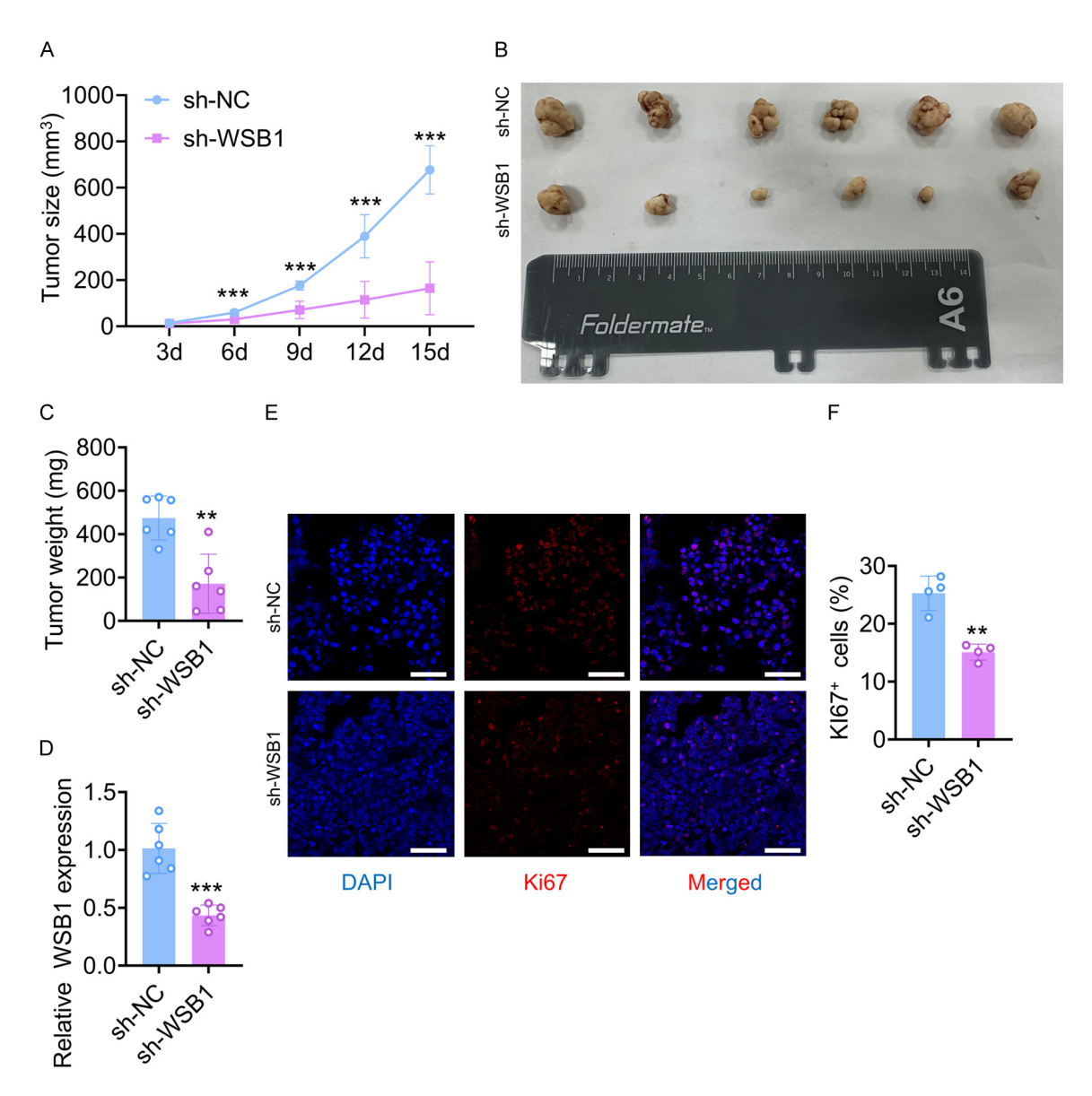


Figure 4. Impact of WSB1 silencing on prostate cancer cell proliferation in vivo. A, B. Tumor volume was significantly reduced in the sh-WSB1 group compared with the sh-NC group. n = 6 per group. C. Tumor weights were compared between sh-NC and sh-WSB1 groups, showing a significant decrease following WSB1 silencing. n = 6 per group. D. WSB1 mRNA expression in xenograft tumors was analyzed by RT-qPCR. n = 6 per group. E. Ki-67 immunofluorescence staining in xenograft tumor tissues were presented. Bar: 50  $\mu$ m; magnification (×200). F. The percentage of Ki-67-positive cells was quantified to evaluate proliferative activity. n = 4 per group. \*\*P < 0.01, \*\*\*P < 0.001.

cantly suppressed in the sh-WSB1 group compared to controls, as evidenced by reduced tumor volume over time (Figure 4A) and smaller tumor sizes upon dissection (Figure 4B). At the study endpoint, tumors from the sh-WSB1 group exhibited markedly lower weights (Figure 4C) and significantly decreased WSB1 mRNA levels, confirming effective knockdown (Figure 4D). Immunofluorescence staining for Ki67, a

marker of cellular proliferation, revealed a substantial reduction in the proportion of Ki67<sup>+</sup> tumor cells in the sh-WSB1 group compared with sh-NC tumors (**Figure 4E**, **4F**), indicating suppressed proliferative activity upon WSB1 depletion. Collectively, these results demonstrate that WSB1 promotes tumor growth in vivo, and its knockdown significantly impairs tumor proliferation and progression.

WSB1 stabilizes ISOC2 by scaffolding its interaction with OTUD4 and preventing ubiquitinmediated degradation

To elucidate the molecular mechanism by which WSB1 regulates prostate cancer progression, immunoprecipitation followed by liquid chromatography-mass spectrometry (IP-LC-MS/MS) was performed to identify WSB1interacting proteins (Figure 5A; Table S1). A total of 106 candidate proteins were identified. among which ISOC2 ranked second based on intensity-based absolute quantification (iBAQ), supporting its potential relevance in WSB1mediated signaling (Figure 5B). Endogenous co-immunoprecipitation assays confirmed a physical interaction between WSB1 and ISOC2 in DU145 and PC-3 cells (Figure 5C). Interestingly, WSB1 knockdown led to a marked decrease in ISOC2 protein levels in both cell lines (Figure 5D), suggesting a regulatory mechanism distinct from the conventional E3 ligase activity of WSB1. Among the proteins identified in the WSB1 interactome, OTUD4, a deubiquitinase, also showed a high iBAO value (Figure 5B), raising the possibility of its involvement in WSB1-mediated regulation of ISOC2. Importantly, WSB1 knockdown did not alter OTUD4 protein levels, whereas WSB1 overexpression increased ISOC2 protein levels without affecting OTUD4 expression (Figure **5E**). These results suggest that WSB1 may function as a scaffold, rather than an enzymatic modifier, to facilitate the interaction between ISOC2 and OTUD4. To examine whether WSB1 regulates ISOC2 protein stability, cycloheximide (CHX) chase assays were performed. ISOC2 degradation was significantly accelerated upon WSB1 knockdown compared to control cells, indicating that WSB1 enhances ISOC2 protein stability (Figure 5F, 5G). Consistently, depletion of OTUD4 led to a reduction in ISOC2 protein levels (Figure 5H), supporting the role of OTUD4 in maintaining ISOC2 stability. In addition, we observed that the addition of MG132 could rescue the effect of WSB1 and OTUD4 on ISOC2 expression (Figure 5I). To further determine whether OTUD4 regulates ISOC2 deubiquitination, ubiquitination assays were conducted. Co-expression of OTUD4 markedly decreased ISOC2 ubiquitination in the presence of HA-Ub-WT and HA-Ub-K48 (Ub with the intact Lys48 residue), but not HA-Ub-K48R (Ub Lys48 residue mutated to Arg), confirming that OTUD4 deubiquitinates ISOC2 in a K48-dependent manner (Figure 5J). Finally, co-immunoprecipitation assays revealed that WSB1 knockdown attenuated the interaction between OTUD4 and ISOC2 (Figure 5K), suggesting that WSB1 stabilizes ISOC2 by acting as a scaffold that facilitates its association with OTUD4. Collectively, these findings identify a previously unrecognized WSB1-OTUD4-ISOC2 axis, wherein WSB1 promotes ISOC2 stabilization by enhancing its interaction with OTUD4 and preventing its ubiquitin-mediated degradation.

Functional silencing of ISOC2 and OTUD4 impairs tumorigenic traits in prostate cancer cells

To investigate the functional role of ISOC2 in prostate cancer, siRNA-mediated knockdown was performed in DU145 and PC-3 cell lines using two independent siRNAs. RT-qPCR confirmed efficient silencing of ISOC2 expression in both cell lines (Figure 6A). CCK-8 assays revealed that ISOC2 knockdown significantly suppressed cell viability (Figure 6B, 6C). Consistently, colony formation assays and transwell migration assays revealed ISOC2 knockdown led to a marked reduction in the number of colonies and reduction in the number of colonies in both cell lines compared to controls (Figure 6D-G).

The functional consequences of OTUD4 knockdown were systematically evaluated in DU145 and PC-3 prostate cancer cells. RT-qPCR confirmed efficient silencing of OTUD4 expression in both cell lines (Figure 7A). Consistent with the findings for ISOC2, CCK-8 assays demonstrated that OTUD4 knockdown significantly reduced cell viability (Figure 7B, 7C). Moreover, colony formation and transwell migration assays revealed a marked reduction in both clonogenic capacity and cell migration upon OTUD4 silencing compared to controls (Figure 7D-G).

The WSB1/OTUD4/ISOC2 axis promotes prostate cancer progression via repression of P16INK4a

Previous evidence suggests that ISOC2 interacts with and suppresses the P16INK4a protein [28]. To determine whether the tumor-suppressive phenotypes induced by disruption of

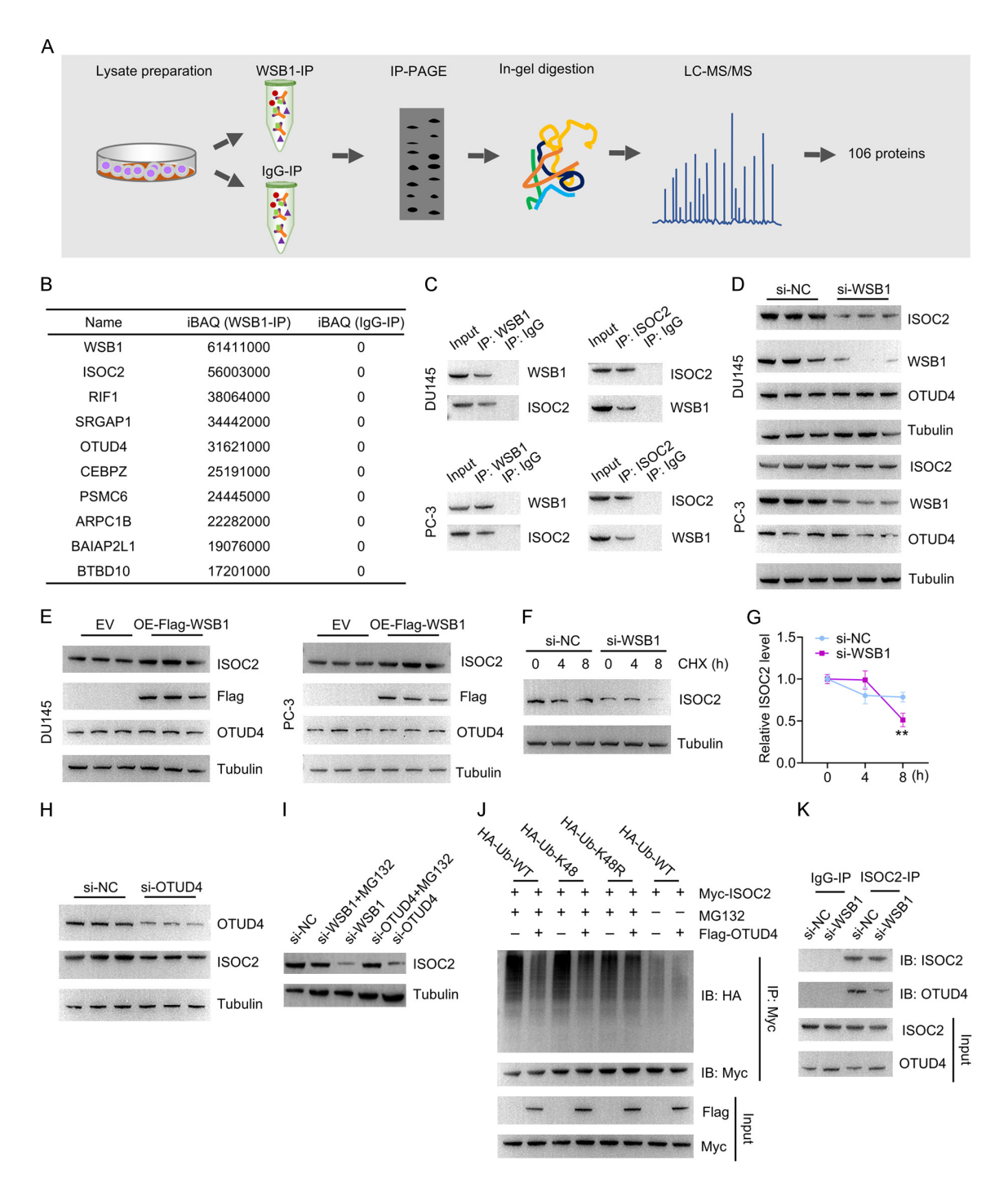


Figure 5. WSB1 interacts with and stabilizes ISOC2 via recruitment of the deubiquitinase OTUD4. A. Schematic of proteomic workflow. B. Top 10 WSB1 interactors identified by IP-MS. C. Co-immunoprecipitation confirms the WSB1-ISOC2 interaction. D. Silencing of WSB1 led to a marked reduction in ISOC2. E. WSB1 overexpression increased ISOC2 protein levels without affecting OTUD4 expression. F, G. Cycloheximide (CHX) chase assays revealed that ISOC2 half-life was significantly shortened upon WSB1 knockdown in PC-3 cells. H. OTUD4 is required for ISOC2 stability. I. Addition of MG132 rescues the effect of WSB1 and OTUD4 on ISOC2 expression. J. Co-expression of OTUD4 markedly decreased ISOC2 ubiquitination in the presence of HA-Ub-WT, HA-Ub-K48 but not HA-Ub-K48R. K. WSB1 knockdown substantially impaired OTUD4 co-association with ISOC2, despite equal input levels, demonstrating that WSB1 scaffolds the ISOC2-OTUD4 complex. \*\*P < 0.01.

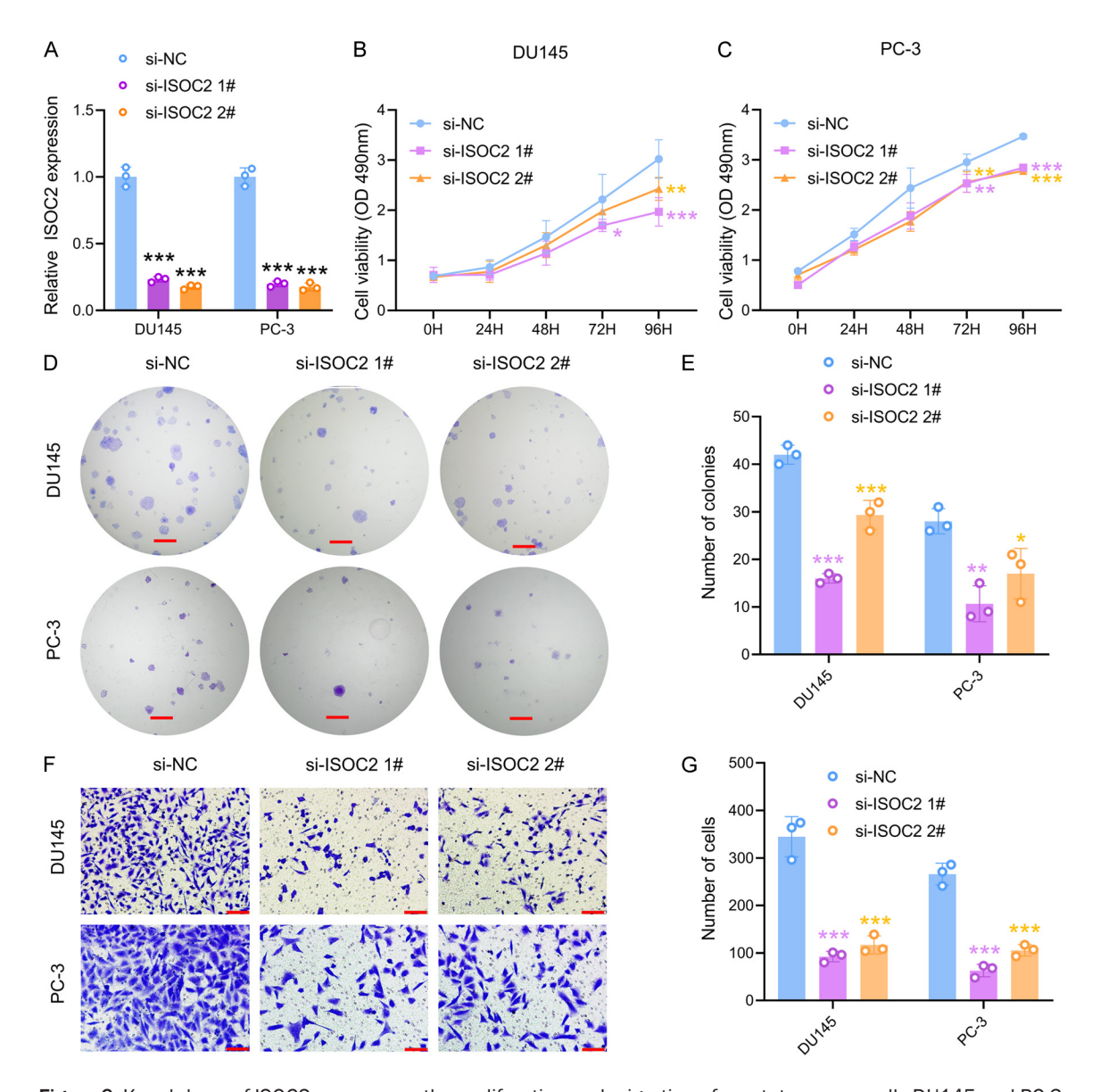


Figure 6. Knockdown of ISOC2 suppresses the proliferation and migration of prostate cancer cells DU145 and PC-3. A. qRT-PCR analysis of ISOC2 mRNA levels in DU145 and PC-3 cells following siRNA-mediated knockdown. B, C. Cell viability was assessed using CCK-8 assays in DU145 and PC-3 cells after ISOC2 knockdown. n = 6 per group. D, E. Colony formation assays were performed to evaluate the clonogenic capacity of DU145 and PC-3 cells. n = 3 per group. Bar: 2 mm; magnification (×1). F, G. Cell migration was assessed using Transwell assays. n = 3 per group. Bar: 100  $\mu$ m; magnification (×200). \*P < 0.05, \*\*P < 0.01, \*\*\*P < 0.001.

the WSB1/OTUD4/ISOC2 axis are mediated through P16INK4a, we performed a series of rescue experiments. While confirming that knockdown of WSB1, OTUD4, or ISOC2 upregulated P16INK4a expression (Figure 8A, 8B) and suppressed malignant phenotypes, we found that co-silencing of P16INK4a significantly restored the proliferative (Figure 8C, 8D), clonogenic (Figure 8E, 8F), and migratory capacities (Figure 8G, 8H) of prostate cancer

cells. Our findings establish that P16INK4a is a critical downstream component through which the WSB1/OTUD4/ISOC2 axis promotes prostate cancer progression.

#### Discussion

A systematic expression analysis of 41 polyubiquitination-related genes in the TCGA prostate cancer cohort was conducted, through

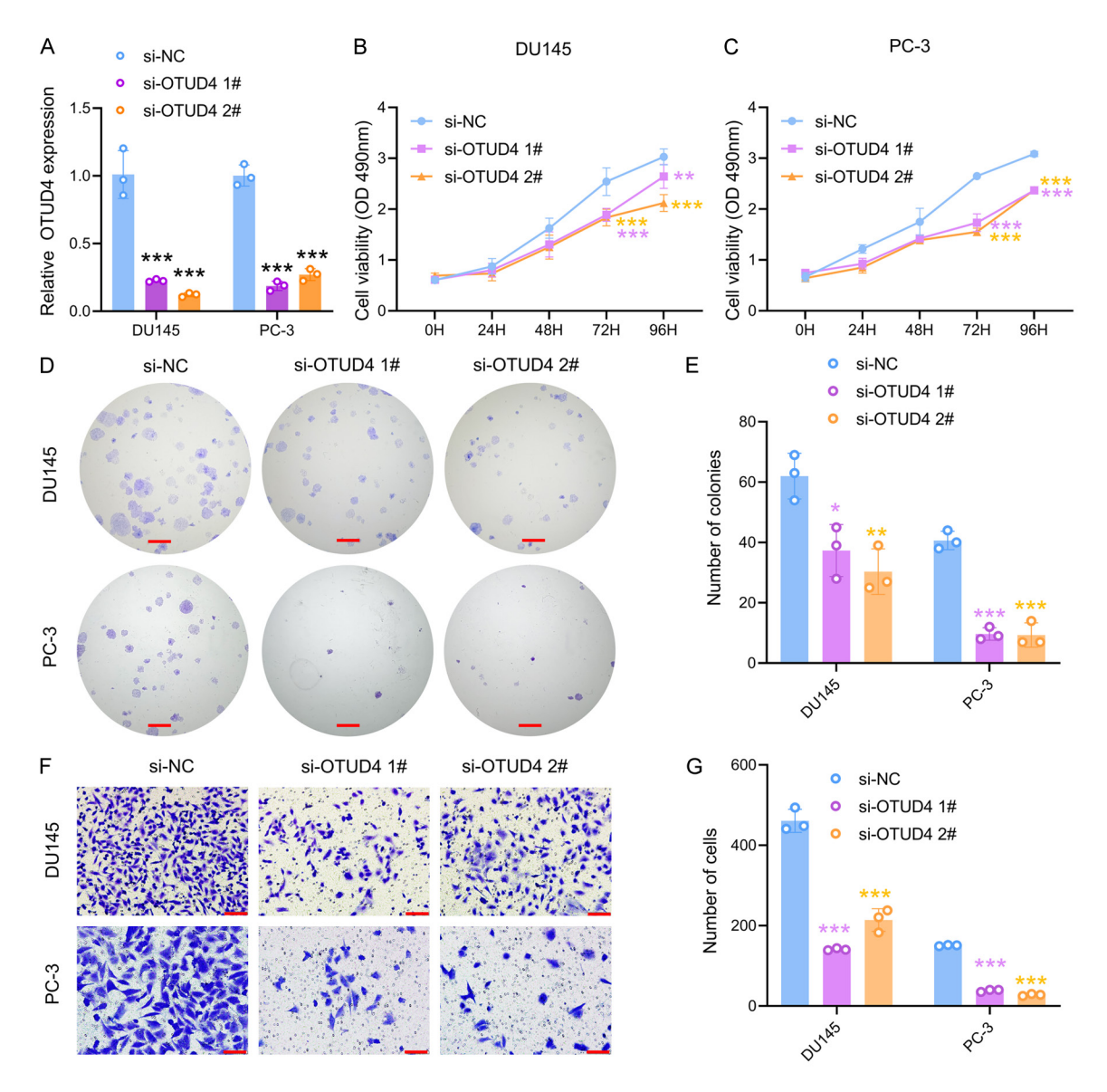


Figure 7. Knockdown of OTUD4 significantly inhibits the proliferation and migration of prostate cancer cells DU145 and PC-3. (A) qRT-PCR analysis of OTUD4 mRNA expression in DU145 and PC-3 cells after siRNA transfection. (B, C) Cell viability was evaluated using CCK-8 assays in DU145 (B) and PC-3 (C) cells following OTUD4 knockdown. n=6 per group. (D, E) Colony formation assays were conducted to examine the effect of OTUD4 knockdown on clonogenic potential; representative images are shown in (D), and quantification in (E). n=3 per group. Bar: 2 mm; magnification (×1). (F, G) Transwell assays were performed to evaluate cell migration. n=3 per group. Bar: 100  $\mu$ m; magnification (×200). \*P < 0.05, \*\*P < 0.01, \*\*\*P < 0.001, \*\*\*\*P < 0.0001.

which 25 genes were identified as significantly dysregulated in tumor tissues. These findings imply that polyubiquitination may potentially contribute to the development of prostate cancer. Among these genes, WSB1 and VHL were upregulated in tumors, and their elevated expression levels were associated with significantly shorter overall survival in affected patients. Subsequent functional experiments demonstrated that WSB1 knockdown resulted

in marked suppression of cell proliferation, colony formation, and migratory capacity in prostate cancer cells. Tumor growth was also inhibited in vivo in xenograft models following WSB1 suppression. Mechanistic investigations revealed that WSB1 acted as a scaffold to facilitate the interaction between the deubiquitinase OTUD4 and its substrate ISOC2, thereby stabilizing ISOC2 protein and preventing its ubiquitin-mediated degradation. This regulato-

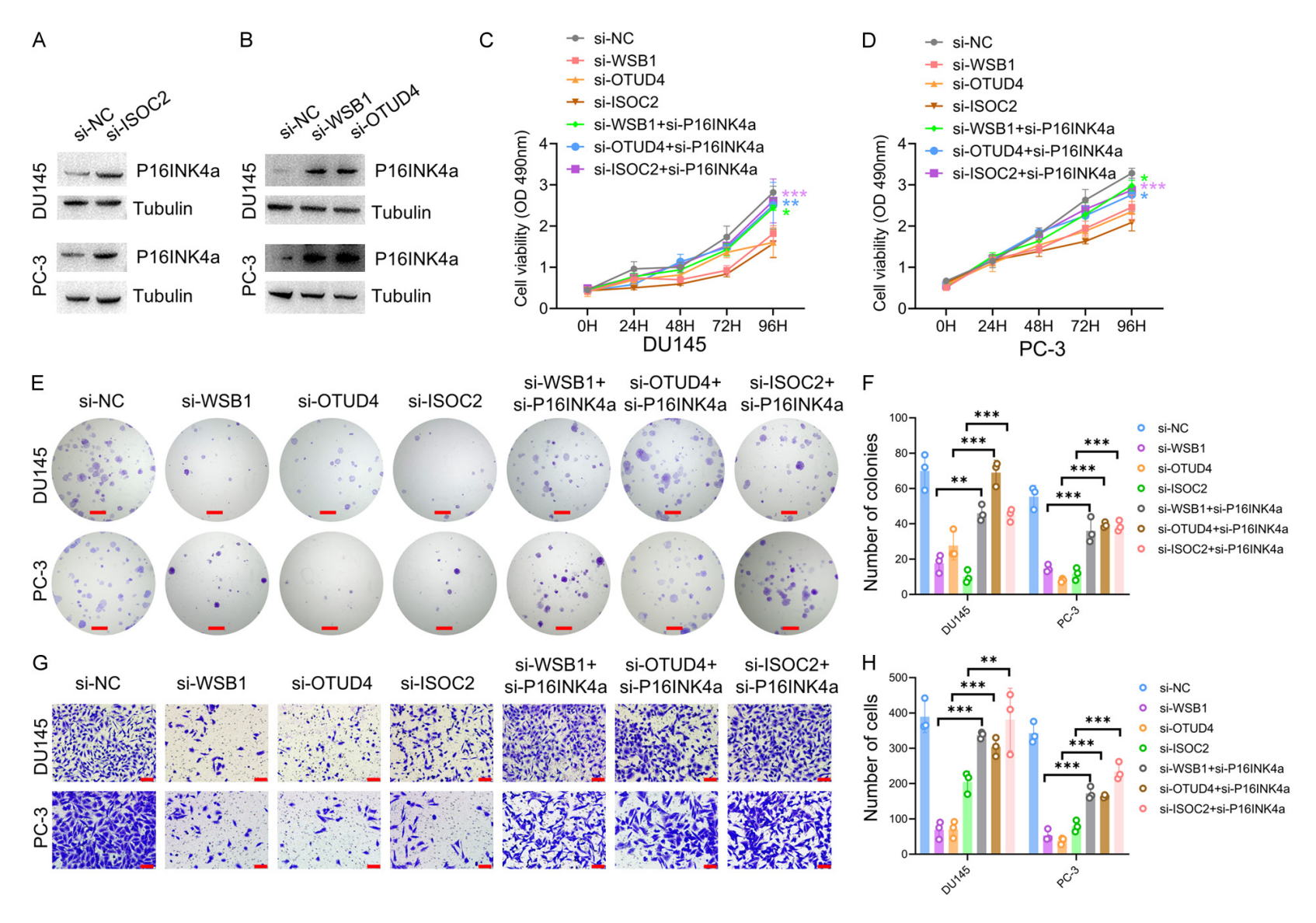


Figure 8. WSB1, OTUD4, and ISOC2 regulate prostate cancer cell proliferation, colony formation, and migration via P16INK4a. A, B. Western blot analysis showed that knockdown of WSB1, OTUD4, or ISOC2 led to upregulation of P16INK4a. C, D. Knockdown of WSB1, OTUD4, or ISOC2 significantly inhibited cell proliferation, which was partially rescued by P16INK4a silencing. n = 6 per group. E, F. WSB1, OTUD4, and ISOC2 silencing reduced colony-forming ability, while co-knockdown with P16INK4a significantly restored colony numbers. n = 3 per group. Bar: 2 mm; magnification (×1). G, H. Knockdown of WSB1, OTUD4, or ISOC2 suppressed cell migration, which was alleviated by co-depletion of P16INK4a. n = 3 per group. Bar: 100 μm; magnification (×200). \*P < 0.05, \*\*P < 0.01, \*\*\*P < 0.001.

ry axis was shown to promote tumor progression by downregulating P16INK4a, thereby relieving cell cycle inhibition.

Ubiquitination has been recognized as a key post-translational modification that broadly regulates cellular processes such as the cell cycle, apoptosis, and signal transduction by modulating the stability, localization, or activity of substrate proteins [7, 29]. In the present study, widespread downregulation of SOCS and ASB family genes was observed, which may impair their negative regulatory functions in oncogenic signaling pathways. For example, SOCS proteins are known to recruit E3 ubiquitin ligase complexes to target cytokine receptors - such as those in the IL-6R/STAT3 pathway - for degradation; loss of SOCS expression may therefore result in sustained STAT3 activation, promoting tumor proliferation and immune evasion [30]. Similarly, ASB family members (e.g., ASB2) have been shown to exert tumor-suppressive effects by targeting components of the Notch signaling pathway for degradation [31]; their downregulation may contribute to the maintenance of cancer stem cell - like traits. In contrast, upregulation of certain genes (e.g., WSB1 and ASB13/14) may promote malignant phenotypes through the ubiquitin-mediated degradation of tumor suppressors or the stabilization of oncogenic proteins. WSB1, for instance, has been reported to stabilize β-catenin via K63-linked ubiquitin chains, thereby activating the Wnt signaling pathway [32]. This bidirectional regulatory mechanism highlights the complexity of the ubiquitin system, whose function depends heavily on substrate specificity, ubiquitin linkage type, and subcellular localization. Therefore, a comprehensive understanding of the dysregulated ubiquitination landscape in prostate cancer requires integrative approaches involving substrate identification and pathway enrichment analyses.

Comprehensive analyses revealed that WSB1 is significantly upregulated in prostate cancer and is closely associated with aggressive clinical features. Functional assays in vitro demonstrated that WSB1 overexpression promotes prostate cancer cell proliferation, colony formation, and motility, whereas depletion of WSB1 produced the opposite effects. In vivo xenograft models further confirmed that modulation of WSB1 expression markedly influences

tumor growth in nude mice. These findings are consistent with previous reports suggesting that WSB1 overexpression promotes tumorigenesis through its E3 ligase activity [15, 33]. However, subsequent mechanistic investigations uncovered a previously unrecognized tumor-promoting mechanism of WSB1. Through immunoprecipitation followed by liquid chromatography-tandem mass spectrometry (IP-LC-MS/MS), 106 WSB1-interacting proteins were identified, among which ISOC2 and the deubiquitinase OTUD4 were highly ranked, indicating a potentially central role in WSB1mediated function. Co-immunoprecipitation (Co-IP) and cycloheximide (CHX) chase assays confirmed physical interactions among WSB1, ISOC2, and OTUD4. Notably, WSB1 knockdown impaired the interaction between OTUD4 and ISOC2. Moreover, OTUD4 was shown to deubiquitinate ISOC2 in a lysine-dependent manner, suggesting that WSB1 functions primarily as a scaffold rather than a catalytic enzyme in this context. Stabilized ISOC2 was found to bind and suppress the cyclin-dependent kinase inhibitor P16INK4a, thereby facilitating cell proliferation. These findings identify OTUD4 and ISOC2 as novel oncogenic factors in prostate cancer, in sharp contrast to their previously limited characterization. While OTUD4 has been minimally studied in prostate cancer, it has been reported to act in a context-dependent manner in other cancers: for instance, OTUD4 overexpression inhibits proliferation and AKT signaling in breast and lung cancers [34, 35], whereas in glioblastoma, OTUD4 was recently shown to promote tumor growth via stabilization of CDK1 and activation of the MAPK pathway [36]. Similarly, ISOC2 has received little attention beyond its reported interaction with P16INK4a [28]. The present study reveals that ISOC2 may function as a downstream oncogenic effector of the WSB1-OTUD4 axis in prostate cancer.

Despite the valuable insights provided by this study, certain limitations remain. While the present work primarily focuses on the role of WSB1 in regulating proliferative and invasive phenotypes of prostate cancer cells, its functions likely extend beyond these aspects. Given the broad involvement of ubiquitination pathways in processes such as DNA damage repair, immune evasion, and therapeutic resistance, WSB1 may also participate in these contexts. For instance, prior studies have demon-

strated that ubiquitin modifications can modulate tumor cell sensitivity to immune checkpoint inhibitors, thereby influencing antitumor immune responses [7]. Moreover, the interaction between WSB1 and hypoxia-inducible factors (HIFs) may reshape the tumor microenvironment by promoting angiogenesis and immune evasion [37]. Notably, the regulation of p16INK4a stability by WSB1 could also impact cellular senescence programs, thereby indirectly altering tumor immunogenicity and immune recognition [38, 39]. These considerations suggest that further investigation into the role of WSB1 in tumor immune regulation, as well as in the development of resistance to androgen deprivation therapy (ADT), holds significant scientific and clinical relevance.

In summary, high expression of WSB1 has been found to be significantly associated with higher Gleason scores and poorer survival outcomes in patients with prostate cancer. A noncanonical oncogenic mechanism of WSB1 has been identified in this study: through its scaffolding function, WSB1 facilitates the interaction between the deubiquitinase OTUD4 and its substrate ISOC2, leading to the stabilization of ISOC2. This stabilization subsequently results in the downregulation of p16INK4a expression, thereby enhancing cellular proliferation and tumorigenicity. It should be emphasized that this mode of action differs markedly from the conventional role of WSB1 as an E3 ubiquitin ligase, suggesting a multifunctional capacity within the ubiquitin signaling network. This atypical mechanism not only broadens the current understanding of WSB1's functional spectrum but also underscores the complexity and plasticity of ubiquitin-mediated regulatory mechanisms in tumor biology.

#### Acknowledgements

We extend our sincere gratitude to Ms. Tiantian Wu for her dedicated care and maintenance of the experimental mouse, which was essential to the successful completion of this study. This work was supported by the Suzhou Clinical Medical Center for Urological Diseases (Szlcyxzx202106).

#### Disclosure of conflict of interest

None.

#### **Abbreviations**

ADT, androgen deprivation therapy; CRPC, castration-resistant prostate cancer; NED, neuro-endocrine differentiation; UPS, ubiquitin-prote-asome system; OS, overall survival; DAPI, 4',6-diamidino-2-phenylindole; siRNAs, Small interfering RNAs; EV, empty vector; CCK-8, Cell Counting Kit-8; LC-MS/MS, Liquid chromatography-tandem mass spectrometry; IP, Immunoprecipitation; CHX, cycloheximide.

Address correspondence to: Gang Li and Xuefeng He, Department of Urology, The First Affiliated Hospital of Soochow University, Suzhou 215000, Jiangsu, China. Tel: +86-18013565283; E-mail: szurol@163.com (GL); Tel: +86-13913163161; E-mail: hxflllove1996@163.com (XFH); Jianjun Xie, Department of Urology, The Affiliated Suzhou Hospital of Nanjing Medical University, Suzhou Municipal Hospital, Gusu School, Nanjing Medical University, Suzhou 215002, Jiangsu, China. Tel: +86-18012603488; E-mail: xjjmobile@njmu.edu.cn

#### References

- [1] Raychaudhuri R, Lin DW and Montgomery RB. Prostate cancer: a review. JAMA 2025; 333: 1433-1446.
- [2] Liu S, Guo H, Li D and Wang C. Immunologically effective biomaterials enhance immunotherapy of prostate cancer. J Mater Chem B 2024; 12: 9821-9834.
- [3] Amaral TM, Macedo D, Fernandes I and Costa L. Castration-resistant prostate cancer: mechanisms, targets, and treatment. Prostate Cancer 2012; 2012: 327253.
- [4] Fan L, Gong Y, He Y, Gao WQ, Dong X, Dong B, Zhu HH and Xue W. TRIM59 is suppressed by androgen receptor and acts to promote lineage plasticity and treatment-induced neuroendocrine differentiation in prostate cancer. Oncogene 2023; 42: 559-571.
- [5] Zhao J, Zhang C, Wang W, Li C, Mu X and Hu K. Current progress of nanomedicine for prostate cancer diagnosis and treatment. Biomed Pharmacother 2022; 155: 113714.
- [6] Johnson RP, Ratnacaram CK, Kumar L and Jose J. Combinatorial approaches of nanotherapeutics for inflammatory pathway targeted therapy of prostate cancer. Drug Resist Updat 2022; 64: 100865.
- [7] Liu F, Chen J, Li K, Li H, Zhu Y, Zhai Y, Lu B, Fan Y, Liu Z, Chen X, Jia X, Dong Z and Liu K. Ubiquitination and deubiquitination in cancer: from mechanisms to novel therapeutic approaches. Mol Cancer 2024; 23: 148.

- [8] Guo H, Su R, Lu X, Zhang H, Wei X and Xu X. ZIP4 inhibits Ephrin-B1 ubiquitination, activating Wnt5A/JNK/ZEB1 to promote liver cancer metastasis. Genes Dis 2024; 11: 101312.
- [9] Guo H, Wei J, Zhang Y, Wang L, Wan J, Wang W, Gao L, Li J, Sun T and Ma L. Protein ubiquitination in ovarian cancer immunotherapy: the progress and therapeutic strategy. Genes Dis 2023; 11: 101158.
- [10] Li X, Li W, Zhang Y, Xu L and Song Y. Exploiting the potential of the ubiquitin-proteasome system in overcoming tyrosine kinase inhibitor resistance in chronic myeloid leukemia. Genes Dis 2023; 11: 101150.
- [11] Zhang S, Guo Y, Zhang S, Wang Z, Zhang Y and Zuo S. Targeting the deubiquitinase USP2 for malignant tumor therapy (review). Oncol Rep 2023; 50: 176.
- [12] Wang J, Liu H, Yu Z, Zhou Q, Sun F, Han J, Gao L, Dou B, Zhang H, Fu J, Jia W, Chen W, Hu J and Han B. Reciprocal regulation between RACGAP1 and AR contributes to endocrine therapy resistance in prostate cancer. Cell Commun Signal 2024; 22: 339.
- [13] Gao Z, Xiong Z, Tao Y, Wang Q, Guo K, Xu K and Huang H. LGR5 interacts with HSP90AB1 to mediate enzalutamide resistance by activating the WNT/beta-catenin/AR axis in prostate cancer. Chin Med J (Engl) 2025; [Epub ahead of print].
- [14] Kile BT, Schulman BA, Alexander WS, Nicola NA, Martin HM and Hilton DJ. The SOCS box: a tale of destruction and degradation. Trends Biochem Sci 2002; 27: 235-241.
- [15] Kim JJ, Lee SB, Jang J, Yi SY, Kim SH, Han SA, Lee JM, Tong SY, Vincelette ND, Gao B, Yin P, Evans D, Choi DW, Qin B, Liu T, Zhang H, Deng M, Jen J, Zhang J, Wang L and Lou Z. WSB1 promotes tumor metastasis by inducing pVHL degradation. Genes Dev 2015; 29: 2244-2257.
- [16] Gao X, You J, Gong Y, Yuan M, Zhu H, Fang L, Zhu H, Ying M, He Q, Yang B and Cao J. WSB1 regulates c-Myc expression through betacatenin signaling and forms a feedforward circuit. Acta Pharm Sin B 2022; 12: 1225-1239.
- [17] Zhang Y, Zhou T, Tang Q, Feng B and Liang Y. Identification of glycosyltransferase-related genes signature and integrative analyses in patients with ovarian cancer. Am J Clin Exp Immunol 2024; 13: 12-25.
- [18] Yang X, He L, Li X, Wang L, Bu T, Yun D, Lu X, Gao S, Huang Q, Li J, Zheng B, Yu J and Sun F. Triptolide exposure triggers testicular vacuolization injury by disrupting the Sertoli cell junction and cytoskeletal organization via the AKT/ mTOR signaling pathway. Ecotoxicol Environ Saf 2024; 279: 116502.

- [19] Wu T, Jin X, Huang C, Yu X, Xu B, Gao W, Qiu X, Bao M, Zhao D, Feng G, Zheng B and Huang X. E3 ligase FBXO22 is not significant for spermatogenesis and male fertility in mice. Am J Transl Res 2024; 16: 1834-1844.
- [20] Hu H, Xi X, Jiang B, Wang K, Wu T, Chen X, Guo Y, Zhou T, Huang X, Yu J, Gao T, Wu Y and Zheng B. RNF187 facilitates proliferation and migration of human spermatogonial stem cells through WDR77 polyubiquitination. Cell Prolif 2025; 58: e70042.
- [21] Wu T, Zhou H, Wang L, Tan J, Gao W, Wu Y, Zhao D, Shen C, Zheng B, Huang X and Shao B. TRIM59 is required for mouse GC-1 cell maintenance through modulating the ubiquitination of AXIN1. Heliyon 2024; 10: e36744.
- [22] Lv J, Wu T, Xue J, Shen C, Gao W, Chen X, Guo Y, Liu M, Yu J, Huang X and Zheng B. ASB1 engages with ELOB to facilitate SQOR ubiquitination and H(2)S homeostasis during spermiogenesis. Redox Biol 2025; 79: 103484.
- [23] Xu BY, Yu XL, Gao WX, Gao TT, Hu HY, Wu TT, Shen C, Huang XY, Zheng B and Wu YB. RNF187 governs the maintenance of mouse GC-2 cell development by facilitating histone H3 ubiquitination at K57/80. Asian J Androl 2024; 26: 272-281.
- [24] Yu X, Xu B, Gao T, Fu X, Jiang B, Zhou N, Gao W, Wu T, Shen C, Huang X, Wu Y and Zheng B. E3 ubiquitin ligase RNF187 promotes growth of spermatogonia via lysine 48-linked polyubiquitination-mediated degradation of KRT36/ KRT84. FASEB J 2023; 37: e23217.
- [25] Yu J, Shen C, Lin M, Chen X, Dai X, Li Z, Wu Y, Fu Y, Lv J, Huang X, Zheng B and Sun F. BMI1 promotes spermatogonial stem cell maintenance by epigenetically repressing Wnt10b/beta-catenin signaling. Int J Biol Sci 2022; 18: 2807-2820.
- [26] Liu Y, Yu X, Huang A, Zhang X, Wang Y, Geng W, Xu R, Li S, He H, Zheng B, Chen G and Xu Y. INTS7-ABCD3 interaction stimulates the proliferation and osteoblastic differentiation of mouse bone marrow mesenchymal stem cells by suppressing oxidative stress. Front Physiol 2021; 12: 758607.
- [27] Kaelin WG Jr. Von Hippel-Lindau disease: insights into oxygen sensing, protein degradation, and cancer. J Clin Invest 2022; 132: e162480.
- [28] Huang X, Shi Z, Wang W, Bai J, Chen Z, Xu J, Zhang D and Fu S. Identification and characterization of a novel protein ISOC2 that interacts with p16INK4a. Biochem Biophys Res Commun 2007; 361: 287-293.
- [29] Kim AH, Chiknas PM and Lee REC. Ubiquitin: not just a one-way ticket to the proteasome, but a therapeutic dial to fine-tune the molecu-

- lar landscape of disease. Clin Transl Med 2024; 14: e1769.
- [30] Handle F, Erb HH, Luef B, Hoefer J, Dietrich D, Parson W, Kristiansen G, Santer FR and Culig Z. SOCS3 modulates the response to enzalutamide and is regulated by androgen receptor signaling and CpG methylation in prostate cancer cells. Mol Cancer Res 2016; 14: 574-585.
- [31] Zhao Y, Li J, Chen J, Ye M and Jin X. Functional roles of E3 ubiquitin ligases in prostate cancer. J Mol Med (Berl) 2022; 100: 1125-1144.
- [32] Long D, Zhang R, Du C, Tong J, Ni Y, Zhou Y, Zuo Y and Liao M. Integrated analysis of the ubiquitination mechanism reveals the specific signatures of tissue and cancer. BMC Genomics 2023; 24: 523.
- [33] Chong L, Zou L, Xiang L, Song X, Miao W, Yan X, Xu M, Ling G, El Agha E, Bellusci S, Lou Z, Zhang H and Zhang JS. WSB1, a hypoxia-inducible E3 ligase, promotes myofibroblast accumulation and attenuates alveolar epithelial regeneration in mouse lung fibrosis. Am J Pathol 2024; 194: 656-672.
- [34] Fan G, Wang F, Chen Y, Zheng Q, Xiong J, Lv Q, Wu K, Xiong J, Wei L, Li D, Zhang J, Zhang W and Li F. The deubiquitinase OTUD1 noncanonically suppresses Akt activation through its Nterminal intrinsically disordered region. Cell Rep 2023; 42: 111916.

- [35] Ma X, Wan R, Wen Y, Liu T, Song Y and Zhu Y. Deubiquitinating enzyme OTUD4 regulates metastasis in triple-negative breast cancer by stabilizing Snail1. Exp Cell Res 2024; 434: 113864.
- [36] Ci M, Zhao G, Li C, Liu R, Hu X, Pan J, Shen Y, Zhang G, Li Y, Zhang L, Liang P and Cui H. OTUD4 promotes the progression of glioblastoma by deubiquitinating CDK1 and activating MAPK signaling pathway. Cell Death Dis 2024; 15: 179.
- [37] Pandey P, Lakhanpal S, Mahmood D, Baldaniya L, Kang HN, Hwang S, Kang S, Choi M, Moon S, Pandey S, Chaudhary K, Khan F and Kim B. Recent update of natural compounds as HIF-1alpha inhibitors in colorectal carcinoma. Drug Des Devel Ther 2025: 19: 2017-2034.
- [38] Safwan-Zaiter H, Wagner N and Wagner KD. P16INK4A-more than a senescence marker. Life (Basel) 2022; 12: 1332.
- [39] Zhang X, Wang J, Tang K, Yang Y, Liu X, Yuan S, Guo F, Zhang L and Ma K. The cell cycle regulator p16 promotes tumor infiltrated CD8(+) T cell exhaustion and apoptosis. Cell Death Dis 2024; 15: 339.